Chemical Science International Journal

30(9): 16-29, 2021; Article no.CSIJ.75576
ISSN: 2456-706X
(Past name: American Chemical Science Journal, Past ISSN: 2249-0205)

Analysis of Agmatine by UV-Visible Absorption Spectrophotometry and Detailed Interference Study on Biogenic Amines and Salts: Grape Application

Khémesse Kital[1,2], Moussa Mbaye[1], Adama Dione[1], Latyr Dione[1], Diéry Diouf[1], Diéne D. Thiaré[1], Lamine Cisse[1], Abdourahmane Khonté[1], Mame D. Gaye-Seye[1], Atanasse Coly[1], Francois Delattre[2] and Alphonse Tine[1*]

[1]Laboratoire de Photochimie et d'Analyse (LPA), Faculté des Sciences et Techniques, Université Cheikh Anta Diop, BP 5005 Dakar, Sénégal.
[2]Laboratoire de Synthèse Organique et Environnement, EA2599, Université du Littoral Côte d'Opale, 145 avenue Maurice Schumann, BP 59140 Dunkerque, France.

Authors' contributions

This work was carried out in collaboration among all authors. This study was designed by authors AT and FD. The experimental work was performed by authors KK, MM, AD, LD, DD, DDT, LC, MDGS and AC drafted the manuscript and interpreted the data. All authors read and approved the final manuscript.

Article Information

DOI: 10.9734/CSJI/2021/v30i930251
Editor(s):
(1) Prof. Francisco Marquez-Linares, Universidad Ana G. Méndez Recinto Gurabo, USA.
Reviewers:
(1) Siamandoura Paraskevi, National Technical University of Athens, Greece.
(2) José Manuel Leao Martins, Vigo University, Spain.
(3) Uta Schnabel, Leib-niz In-sti-tu-te for Plas-ma Sci-ence and Technology, Germany.
Complete Peer review History: http://www.sdiarticle4.com/review-history/75576

Original Research Article

Received 13 August 2021
Accepted 27 October 2021
Published 01 November 2021

ABSTRACT

The aim of this work is to develop a new method for the analysis of agmatine from UV-Visible absorption spectra. The optimization of the analytical parameters shows that the stoichiometry of the orthophthalaldehyde-agmatine complex is 1:1, the optimal pH is equal to 11 and the stability time is about 10 minutes. The analytical performances obtained are satisfactory with very low limit of detection (LOD) and limit of quantification (LOQ) respectively equal to 0.121 µg/mL and 0.405 µg/mL. The relative standard deviation (RSD) obtained of 2.1% shows the good reproducibility of the measurements. Interference effects show that the aromatic biogenic amines interfere less than linear ones, excepted serotonine. Similarly, a more marked interference is found for chloride salts.

**Corresponding author: E-mail: alphtine@yahoo.fr;*

Finally, a recovery rate of between 99.4% and 111.7% was found in the grape extract studied, showing the effectiveness of the method.

Keywords: UV-Visible; spectrophotometry; agmatine; orthophthalaldehyde; grape.

1. INTRODUCTION

Biogenic amines are low molecular weight organic bases found in most foods. Some amines have aromatic structures (tyramine, dopamine, 2-phenylethylamine) and others aliphatic (agmatine, putrescine, spermine, and spermidine). These amines are produced largely by the microbial decarboxylation of amino acide. This formation depends on a specific bacterial source [1]. At high doses, biogenic amines become toxic. Symptoms may vary depending on the biogenic amine and the sensitivity of the subject [2, 3]. Agmatine, was discovered in 1910 by Albrecht Kossel in herring sperm [4]. In the human body, it is synthesized and stored in astrocytes [5] then transported to the cerebral nerve endings [6]. It is produced from L-arginine through the action of the enzyme arginine decarboxylase (ADC) [7, 8]. However, in the presence of enzymes such as agmatinase or diamine oxidase, agmatine can be transformed into putrescine or 4-guanidinobutanal respectively [9-11]. Agmatine also has a wide range of activities related to nervous system functions [12-14]. Indeed, it acts as a potential neurotransmitter in the brain [15, 16] by regulating for example the level of polyamines [17]. In addition, it reduces collagen accumulation in diabetics [18], plays a protective role against depression in mice [19] and regulates epithelial cell growth for wound healing [20]. It also increases muscle growth while improving physical fitness [21]. This is why the presence of agmatine in the body is of great interest. Indeed, its presence in foods such as meat, fish and cheese serves as a chemical indicator of their hygienic quality [22].

Despite these beneficial effects, the consumption of agmatine in large quantities has adverse effects including gastrointestinal distress, mild diarrhea with vomiting and nausea [23].

Thus, several analytical methods have been developed for the determination of agmatine in food products. Among these, high performance liquid chromatography (HPLC) coupled with a UV-visible or fluorescence detector is the most widely used [24-29]. Nowadays, spectrofluorimetric analysis of agmatine has proven to be one of the most efficient [30-32]. While agmatine absorbs weakly in the visible range, its derivative with several markers such as orthophthalaldehyde (OPA), benzoyl chloride, (ClB), 4-fluoro-7-nitro-2,1,3-benzoxadiazaole (FNBD), 2,3-naphthalenedialdehyde (NDA) yields complexes with high molecular extinction coefficients (ϵ) at least in the UV-visible range [33-34]. These methods are very expensive and require qualified personnel for implementation. For these reasons, it is necessary to develop other methods less expensive and very easy to implement with realible sample preparation procedures before instrumental analysis which lead to achieve an analytical method more precise and accurate. To our knowledge, no studies on the determination of agmatine by UV-visible absorption from its complex with a label have been found.

Thus, the aim of the present work is to develop a new method for the analysis of agmatine by UV-visible molecular absorption spectrophotometry. After optimizing the analytical parameters (stoichiometry, pH and stability time), the analytical performance was determined. Prior to any application in grape, a detailed study of the interference effects with other biogenic amines and salts likely to be present in the food matrix was examined.

2. MATERIALS AND METHODS

2.1 Reagents and Chemicals

Agmatine sulfate (AGM), 97% pure, orthophthalaldehyde (OPA), 97% pure, hydrochloric acid (HCl), 37% pure, sodium hydroxide (NaOH), 98% pure and demineralized water were used. All products are of analytical quality and were supplied by Sigma-Aldrich (Taufkirchen, Allemagne).

2.2 Apparatus

Absorption spectra were recorded using a cary 100 spectrophotometer scanning between 190 and 900 nm with a variable pass band of 0.2 to 4 nm. This apparatus includes two cells, one for the solvent and the other for the sample.

Absorbance measurements were made using two quartz cuvettes with two polished sides (1 cm optical path). Weighing was done using a Sartorius balance with a precision of 0.1 mg. A Consort C6010 pH meter and a SL16R thermo scientific centrifuge were used. The different software used were: WinUV for recording absorption spectra and OriginPro 8.5 for data processing.

2.3 Procedure

Agmatine (AGM) and orthophthalaldehyde (OPA) stock solutions of 10^{-2} M concentration each were prepared in 25 mL volumetric flask in aqueous medium. From each stock solution, dilutions were made to obtain the desired concentration of daughter solutions. The solutions were protected from light with aluminium foil and stored in a refrigerator at 277 K.

500 g of fresh grapes were crushed and decanted. 10 mL of the liquid obtained after decanting was placed in a tube and centrifuged at a speed of 5000 rpm for 10 minutes, then the supernatant was filtered through a whatman filter paper. The filtrate obtained was then protected with aluminium foil and stored in the refrigerator until use. Prior to any measurement, 1 mL of this filtrate was diluted one-tenth in demineralized water.

3. RESULTS AND DISCUSSION

3.1 Identification of the Absorption Spectrum of the OPA-AGM Complex

For the respective concentration of $8x10^{-5}$ M, agmatine and OPA absorb weakly in UV visible range. However, mixing OPA with AGM results in a complex that absorbs significantly in the visible range with two maxima located at 269 nm and 328 nm (Fig. 1).

3.2 Optimization of Analytical Parameters

3.2.1 Determination of the stoichiometry of the complex between OPA and AGM

The stoichiometry of the complex is determined from the intersecting point of the two straight lines translating the evolution of the absorbance of the complex according to the concentration of one product, the other remaining invariable. In our case, the stoichiometry of the OPA-AGM complex was studied in aqueous medium (pH 11).

Initially, the concentration of OPA was set at 10^{-4} M and that of agmatine varied from $2x10^{-5}$ M to $2x10^{-4}$ M. The variation of the absorbance of the complex versus agmatine concentration shows two intersecting straight lines with distinct slopes (Fig. 2A). The first line has a positive slope and indicates the formation of the complex; the second line has a negative slope and indicates that agmatine inhibits the absorbance of the complex. The point of intersection of the two straight lines corresponds to the end of the reaction. At this point, the concentration of agmatine is equal to that of the fixed OPA; this indicates that the stoichiometry of the complex is 1:1.

A second experiment was carried out, this time fixing the concentration of AGM at 10^{-4} M and varying the concentration of OPA from $2x10^{-5}$ M to $2x10^{-4}$ M (Fig. 2B). This figure shows two intersecting straight lines. Their point of intersection marks the end of the complex formation; this also confirms the existence of a 1:1 complex. Beyond this point, the excess of OPA exalts the absorption of the complex.

In all cases, no change in spectral shape or wavelength shift was observed throughout the experiment. This 1:1 stoichiometry found is consistent with the result obtained in fluorescence [30].

3.2.2 pH effect on the absorption spectra of the OPA-AGM complex

pH is an important factor that can affect the structure of a molecule by causing electron delocalization with a chemical shift of bonds [35]. This change in structures can therefore affect the absorption spectrum of the molecule either in intensity or in wavelength shift. To study the effect of pH on the absorption of the OPA-AGM a concentration of $2x10^{-4}$ M of this complex was used in a pH range of 1 to 14. For each pH value, the absorption spectrum was recorded and the intensity of the maximum peak determined. No significant change in the shape of the spectra was observed, other than a small wavelength shift (2 nm) when moving from pH 11 to pH 14. From the maximum absorption intensities (AI) at 328 nm, the variation curve AI = f (pH) was plotted (Fig. 3). This figure shows a very low absorbance in acidic medium. However, in alkaline medium, a remarkable increase in

absorption intensity is observed, with a maximum at pH 11. This figure shows that the absorbance intensity of the OPA-AGM complex increases progressively to a maximum at pH 11 (Fig. 3). This result shows that the optimal pH is equal to 11 and this pH value was then chosen for the rest of the work.

3.2.3 Study of the stability of the OPA-AGM complex

The stability of the OPA-AGM complex ($18x10^{-5}$M) in aqueous medium (pH 11) was studied by following the evolution of the absorption signal at 328 nm over time from the beginning of the

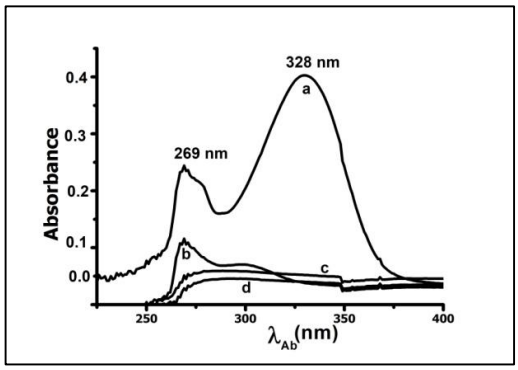

Fig. 1. Different absorption spectra in aqueous medium (pH = 11) (a) OPA-AGM; (b) OPA; (c) AGM and (d) solvent

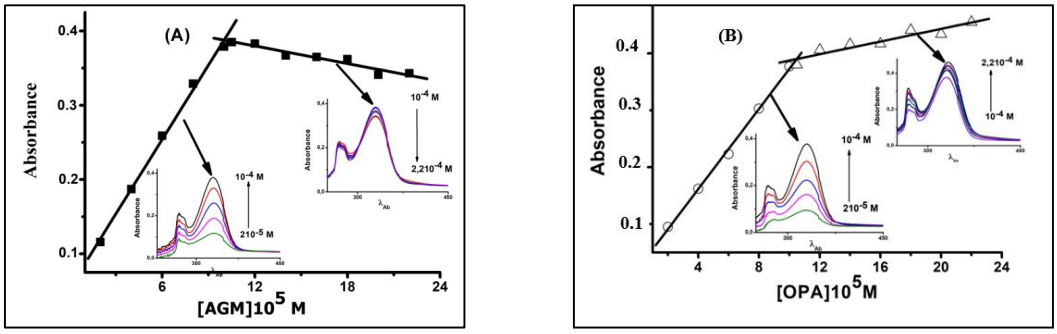

Fig. 2. Evolution of the absorbance of the OPA-AGM complex depending on the concentration: AGM (A) and OPA (B); *(λ_{max} = 328 nm; pH = 11)*

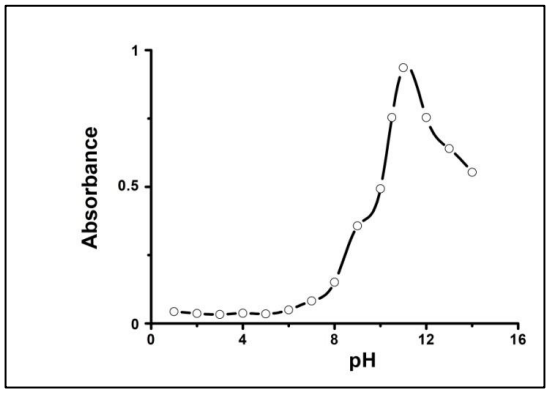

Fig. 3. pH effect on the absorbance of the OPA-AGM complex

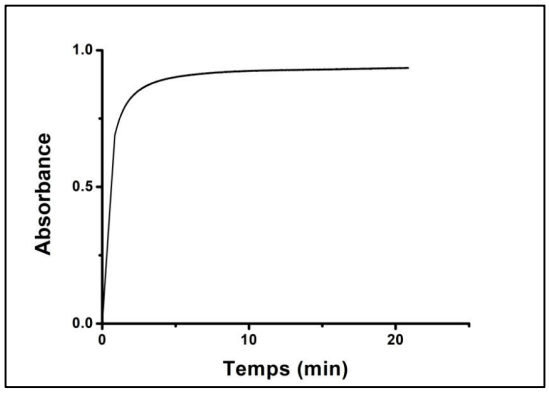

Fig. 4. Stability data of OPA-AGM complex (λ_{max} = 328 nm; pH = 11)

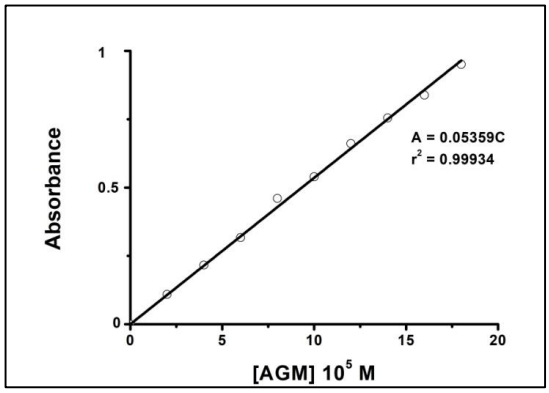

Fig. 5. Calibration for the OPA-AGM complex in aqueous medium (λ_{max} = 328 nm, pH 11)

mixing (Fig. 4). The complex formed between OPA and agmatine starts to stabilize after 5 minutes and at about 20 minutes the complex appears to be completely stable (Fig. 4). Thus, the stabilization time is shorter in absorption than in fluorescence [36].

3.3 Calibration Curve and Analytical Performance

In order to better appreciate the interest of this method, the calibration of the OPA-AGM complex in water was established from the absorption peak maxima, while respecting the optimal conditions at pH 11 (Fig. 5). We noted a good linearity of the straight line with a correlation coefficient higher than 0.999. From this line, the analytical performances were determined: the limit of detection (LOD), the limit of quantification (LOQ) and the relative standard deviation (RSD).

The slope ($\alpha = 0{,}0536 \pm 0{,}0004$) of this straight and the standard deviation (σ_s) of the absorbance of the solvent allowed us to determine the analytical performance using the following equations:

$$\mathrm{LOD} = \frac{3\sigma_s}{\alpha}$$

$$\mathrm{LOQ} = \frac{10\,\sigma_s}{\alpha}.$$

Thus, we obtained limits of detection of 0.121 µg/mL and of quantification equal to 0.405 µg/mL. These low limit values show the good sensitivity of the method. In addition, the relative standard deviation of 2.1 % found attests to the good reproducibility of the measurements.

Thus, our method is sensitive and reproducible. This new method can be applied to the analysis of agmatine in different matrices. However, most biogenic amines in the presence of OPA absorb in the same area as the OPA-AGM complex, which can cause important interference effects according to the amine.

3.4 Interference Study

3.4.1 Interference with biogenic amines

In this study we were interested in biogenic amines with a primary amine group such as histamine (HIST), spermidine (SPD), cadavérine (CAD), putrescine (PUT), dopamine (DOPA), serotonine (SERO), tyramine (TYR) and tryptamine (TRYP). In fact, these amines are present in many foods (plant and fish products) [37-41] and can complex with OPA giving a more or less important absorbance in our studied wavelength range (Fig. 6). Moreover, some of these absorption spectra show more or less large overlaps with the absorption band of the OPA-AGM complex at around 328 nm (Fig. 6). This figure shows a large overlap of the absorption band of the OPA-PUT complex with OPA-AGM. However, with histamine there is a more or less marked overlap. Thus, histamine will interfere less than putrescine in the determination of agmatine. In any case, it is therefore necessary to determine the tolerance limits of these biogenic amines before any analysis of agmatine in food products.

To determine tolerance limits, the effect of the concentration of these amines on the absorbance of the OPA-AGM complex was evaluated. For this purpose, the concentration of agmatine and OPA were set respectively at $1.2x10^{-4}$ M and 10^{-3} M, while that of the interfering agent varied between $0.2x10^{-4}$ M and $2x10^{-4}$ M (Fig. 7). This figure shows that, in general, the absorbance of the OPA-AGM complex increases progressively with the concentration of the added amine. This figure 7 shows that serotonine, spermidine, putrescine, dopamine and cadaverine already admit remarkable interference for a concentration equal to one fifth of that of agmatine. On the other hand, for respective concentrations of tyramine, tryptamine and histamine of between 0 and 100% of that of agmatine used, their presence has very little influence on the absorbance of the OPA-AGM complex.

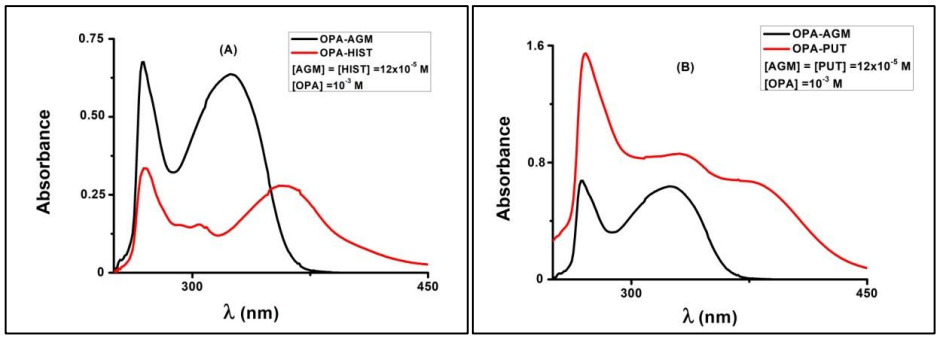

Fig. 6. Superposition of the absorption spectra of the OPA-AGM complex with the other OPA-amine complexes: OPA-AGM and OPA-HIST (A); OPA-AGM and OPA-PUT (B)

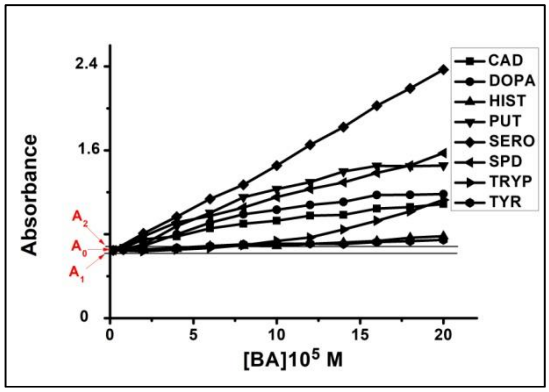

Fig. 7. Effect of biogenic amines (BA) on the absorbance of OPA-AGM complex

Table 1. Tolerance limits (TL) and corresponding mass rates according to the range of the added biogenic amine

Biogenic amines	Tested Concentration Ranges (µg/mL)	LT (µg/mL)	$*\tau(\%$ by mass$)$
Tryptamine	3.204 – 28.840	15.591	56.9
Histamine	3.681 – 29.451	12.656	46.2
Tyramine	3.204 – 28.436	11.299	41.2
Dopamine	1.517 – 28.549	4.075	14.9
Putrescine	1.289 – 28.993	3.349	10.2
Cadaverine	1.401 – 28.016	2.111	7.7
Spermidine	0.509 – 28.328	1.497	5.5
Serotonine	0.425 – 29.775	1.267	4.6

$* \tau(\%\ \text{By mass}) = \frac{[AB]}{[AGM]_0}.100$ with $[AGM]_0 = 27.392 \mu g/mL$

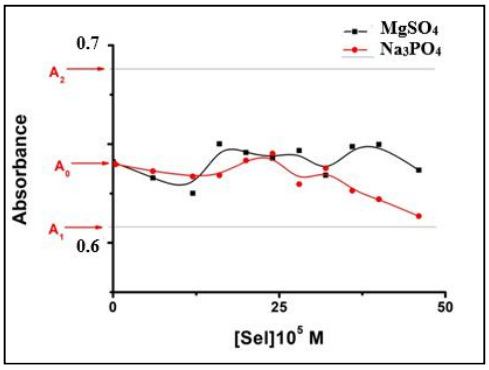

Fig. 8. $MgSO_4$ and Na_3PO_4 effect on the absorbance of the OPA-AGM complex

From the variation of the absorbance versus concentration of the interfering amine, it was possible to determine the tolerance limits (TL) for each amine. In our case, the tolerance limit was defined as the concentration limit for which the percentage variation of the absorbance of the OPA-AGM complex does not exceed ± 5%.

Thus we can write:

$$\Delta = \pm 5\% = \frac{A_0 - A}{A_0} \Leftrightarrow \pm 5 = \frac{A_0 - A}{A_0} \times 100$$

In this expression A_0 is the absorbance of the complex alone and A that of the complex in the presence of the corresponding amine. Thus, there are two limit values of A noted A_1 and A_2 corresponding to this precision.

If Δ is positive, in which case A is less than A_0 (extinction), we have: $A_1 = \frac{95A_0}{100}$

If Δ is negative, in this case A is greater than A_0 (exaltation) we have: $A_2 = \frac{105A_0}{100}$

The intersection of the curve $A = f([AB])$ with the straight lines $y = A_1$ and $y = A_2$ correspond to the tolerance limits x_1 or x_2 respectively. If there is no intersection, the amine does not interfere with the determination of agmatine, with respect to prefixed precision. In this section the concentrations are expressed as mass concentrations. All the results are grouped in the Table 1.

Taking into account the limits of tolerance or mass levels in relation to agmatine, this table shows that in absorption, serotonine interferes much more in the determination of agmatine, followed by spermidine, then cadaverine, putrescine and finally dopamine. However, there was little interference for tyramine, histamine and tryptamine in the determination of agmatine in absorption. These results are consistent with the observations obtained experimentally (Fig. 6 and 7). Indeed, the differences noted on the tolerance limits or mass rates from one amine to another can be explained by the possible existence of overlapping absorption bands around 328 nm with that of the OPA-AGM.

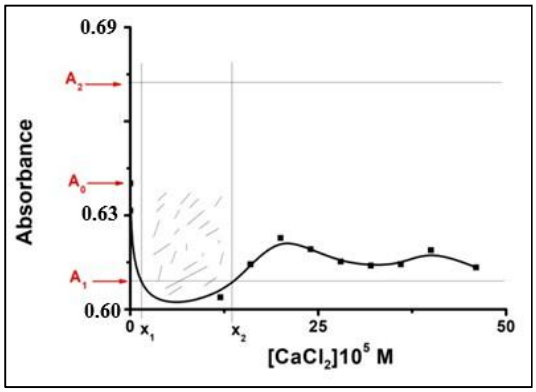

Fig. 9. Effect of $CaCl_2$ on the absorbance of the OPA-AGM complex

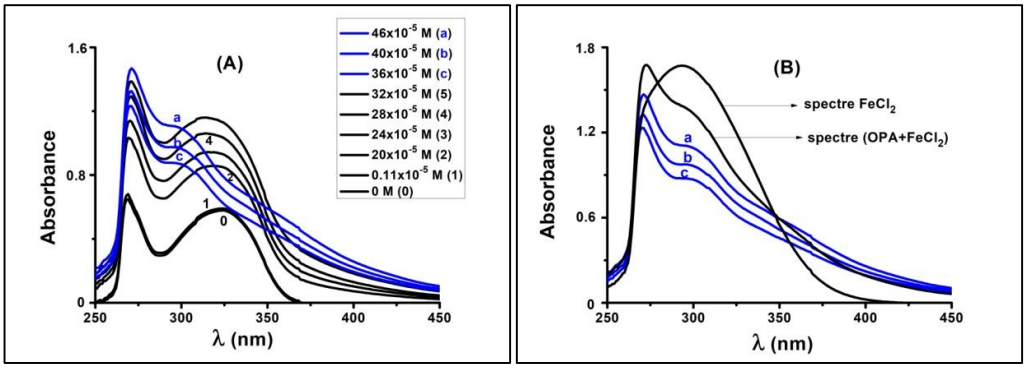

Fig. 10. $FeCl_2$ effect on the absorption spectrum of the OPA-AGM (A); Comparison of the absorption spectra a, b and c with that of $FeCl_2$ in water and the $FeCl_2$ in OPA solution (B)

3.4.2 Interference with salts

Most salts likely to be present in food matrices are: $CaCl_2$, $MgSO_4$, NaCl, Na_3PO_4 and $FeCl_2$ [42]. Therefore, their respective influence on the absorption of the OPA-AGM complex at the wavelength of 328 nm was investigated. In this study we were able to determine for each salt its tolerance limit and its corresponding mass ratio. These tolerance limits and mass ratios are calculated in the same way as those for biogenic amines. However, with the amines the influence of the interfering on the absorbance of the OPA-AGM complex was linear and increasing, this is not the case with the salts. Indeed, the shape of the curve of variation of the absorbance versus concentration of the salt evolves from one salt to another. This is why this study will be carried out on a case by case basis according to the salt.

For the salts $MgSO_4$ and Na_3PO_4 no intersection of the lines $y = A_1$ and $y = A_2$ with the evolution of the absorbance with respect to salt concentration has been observed (Fig. 8). They therefore have no influence on the determination of agmatine, at least on the range used.

For the $CaCl_2$ salt, Fig. 9 shows that the presence of the salt does not enhance the absorbance of the complex, but rather inhibits it. However, the curve of the evolution of the absorbance with respect to salt concentration intersects the line $y = A_1$ at two points of respective concentrations x_1 (2.32 µg/mL) and x_2 (19.54 µg/mL) corresponding to the tolerance limits of $CaCl_2$. Taking into account the shape of this curve and the values of x_1 and x_2, an accuracy of less than 5% can be obtained only for concentration ranges $0 < °C < x_1$ et $x_2 < C < 67.62$. The agmatine level can however be measured between x_1 and x_2 but with an accuracy of more than 5%.

For $FeCl_2$, the study of this salt effect on the absorbance of the OPA-AGM complex shows a certain peculiarity on the shape of the absorption spectrum versus its concentration (Fig. 10A). For a salt concentration between 0 and $36x10^{-5}$ M,

there is an exaltation of the absorbance with no change on the shape of the spectrum. Above this level there is a large change on the shape of the absorption spectrum of the OPA-AGM complex with a fall in absorbance at this wavelength. This $36x10^{-5}$ M concentration of the salt corresponds to three of the agmatine concentration used. Comparison of the spectra (a, b and c) in figure with that of the OPA-$FeCl_2$ mixture (Fig. 10B) shows the same spectral patterns. Thus, for a salt concentration three times higher than that of agmatine, there is a break in the OPA-AGM complex in favor of the complex between OPA and $FeCl_2$. Above a concentration of $FeCl_2$ three times higher than that of AGM, the complex obtained is not OPA-AGM.

With these remarks in mind, the tolerance limits were determined. The variation of the absorbance of the complex with respect to salt concentration is shown in Fig. 11. This figure shows that the presence of $FeCl_2$ exalts the absorbance of the complex. This exaltation passes through a maximum at the salt concentration equal to 86.4 µg/mL (zone 2, Fig. 11). Thus, given the shape of this curve, two values should be found corresponding to the intercept of this curve with the line $y = A_2$: a first value calculated from the rising branch and a second value on the falling branch. The rising branch intersects the line $y = A_2$ at concentration x_1 = 9.63 µg/mL. However, at three times the molar concentration of salt, the 328 nm band of the complex disappears in favor of the formation of another complex (zone 3, Fig. 11). Thus, to be accurate in the determination of the OPA-AGM complex in the presence of $FeCl_2$, the salt concentration should not exceed 9.63 µ g/mL, which means 35.1% $FeCl_2$ by mass only relation to AGM. Thus, in the presence of the $FeCl_2$ salt, the determination of AGM in OPA solution can be done with an accuracy of less than 5% only in zone 1 of Fig. 11.

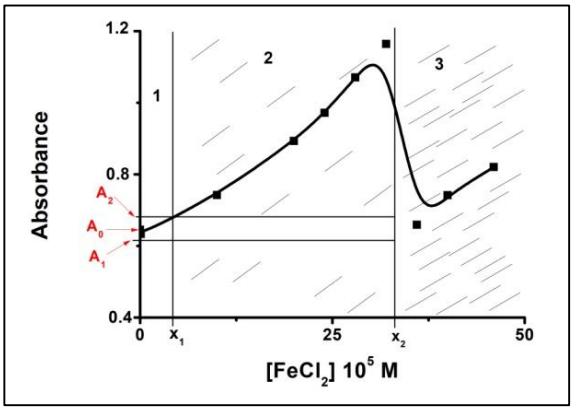

Fig. 11. $FeCl_2$ effect on the absorbance of the OPA-AGM complex

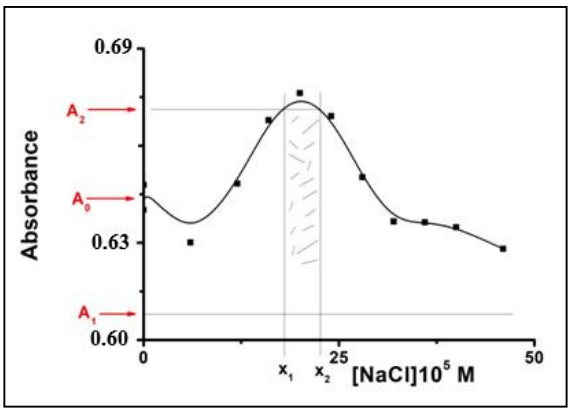

Fig. 12. Effect of NaCl on the absorbance of OPA-AGM complex

Table 2. Tolerance limits (TL) and corresponding mass rates according to the range of added salt

Salts	Tested concentration range (µg/mL)	LT ($\mu g/mL$)	$\tau(\%\ by\ mass)*$
$CaCl_2$ (Ca^{2+}, $2Cl^-$)	0.0147-67.62	2.32-19.54	8.5-71.3
$FeCl_2$ (Fe^{2+}, $2Cl^-$)	0.027-124.20	9.63	35.2
$MgSO_4$ (Mg^{2+}, SO_4^{2-})	0.0171-78.66	∞	∞
NaCl (Na^+, Cl^-)	0.0058-28.68	10.44-12.97	38.1-47.4
Na_3PO_4 ($3Na^+$, PO_4^{3-})	0.664-76.36	∞	∞

$* \tau(\%\ by\ mass) = \frac{[Sel]}{[AGM]_0}.100$ *Fixed agmatine concentration equal to 27.392* $\mu g/mL$

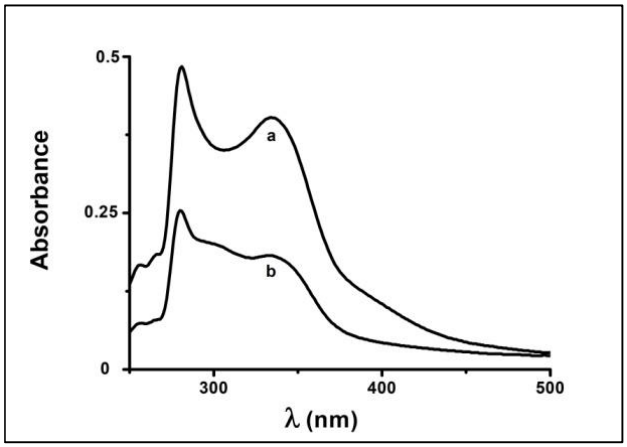

Fig. 13. Absorption spectra of OPA-AGM (a) and extract-OPA mixture (b)

For the NaCl salt, no effect on the shape of the absorption spectrum of the OPA-AGM complex was observed with respect to salt concentration. However, the absorbance versus NaCl concentration has an ascending and descending branch with a maximum at 11.7 $\mu g/mL$ (Fig. 12). The straight line y = A_2 intersects this curve at two points x_1 (10.44 $\mu g/mL$) and x_2 (12.97 $\mu g/mL$) (Fig. 12). Thus, for NaCl concentrations below 10.44 $\mu g/mL$ or above 12.97 $\mu g/mL$, agmatine can be determined with an accuracy of 5%. Between the two concentrations agmatine can still be determined but with higher accuracy. Thus, for mass ratios of NaCl to agmatine of less than 38.1% and greater than 47.4% respectively, agmatine can be determined with an accuracy of at least 5%.

All the results of this interference study are summarized below in Table 2.

3.5 Application on Red Grapes

Before quantifying agmatine in grapes, we first started to prove its presence in the grapes used.

3.5.1 Detection of agmatine in grape

To show the existence of agmatine in the grape extract, in the presence of an excess of OPA, a comparative study of the absorption spectra of the standard agmatine solution and the extract was made under the same conditions at pH 11 (Fig. 13). This figure shows both the extract and the standard solution of agmatine, the existence of two peaks located respectively at around 269 nm and 328 nm. In both cases the peak at 328 nm has a lower intensity. The absorption bands of the two solutions (standard and grape extract) are thus superimposed. This confirms the presence of agmatine in the grape. However, for the absorption spectrum of the extract, a weak shoulder can be seen at around 303 nm. The existence of this shoulder shows that our extract would contain more or less other biogenic amines in addition to agmatine.

3.5.2 Quantitative analysis of agmatine in grape

To determine the amount of agmatine in the grape extract, the standard addition curve was

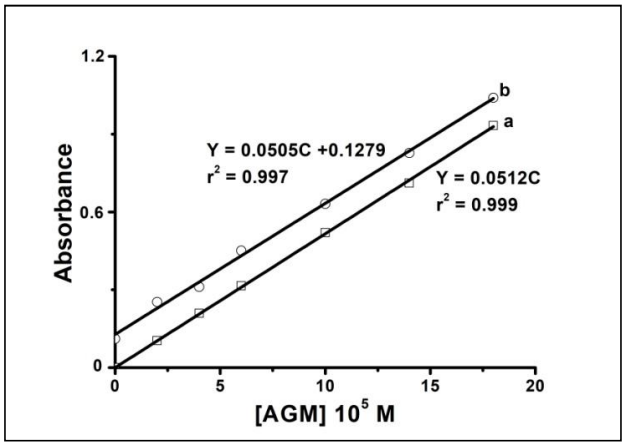

Fig. 14. Curves of agmatine calibration (a) and standard addition of grape extract (b)

Table 3. Evaluation of the percentage recovery of agmatine in grape extract

Type of sample	Added (Ca) (μg/mL)	Found (Ct) (μg/mL)	Recovery (%R)	RSD (%)
	0	5.02	-	
	4.57	10.71	111.7	
	9.13	14.11	99.7	
grape	13.69	19.61	103.3	1.9
	22.83	27.89	100.1	
	31.96	36.77	99.4	

established. This curve is almost parallel to the calibration of agmatine (Fig. 14).

This good parallelism shows that the matrix effect is very negligible in all our measurements. From this curve, recovery percentage (% R) was determined using the following formula:

$$\%R = \frac{C_t}{C_0 + C_a} \times 100.$$

In this relationship, C_t represents the concentration of agmatine found, C_a the added concentration and C_0 the blank concentration.

In this extract, very satisfactory recovery percentages between 99.4% and 111.7% were found (Table 3). These values close to 100% show the efficiency of the extraction method. Similarly, the low value of the relative standard deviation equal to 1.9% shows the good reproducibility of the measurements.

These values found are therefore in accordance with international standards for the validation of analytical methods.

4. CONCLUSION

In this work, we determined low detection limits and low quantification limits, indicating the good sensitivity and precision of this method. Also, the low relative standard deviation found shows the good reproducibility of the measurements. Also, this study shows that some biogenic amines and some salts interfere more or less well with agmatine. However, the parallelism obtained between the curves of standard addition and the calibration shows that interference effects are very insignificant when determining agmatine in grape. Thus, very satisfactory recovery percentages for the analysis of agmatine in grape extract were found. All this shows the efficiency of analysis method of agmatine by UV-Visible spectrophotometry.

Thus, in this work, simple, sensitive, accurate analytical method by UV-Visible spectrophotometry for the determination of agmatine was optimized. In addition, this method is note expensive. Therefore, it can be proposed for the analysis of agmatine in many food samples.

DISCLAIMER

The products used for this research are commonly and predominantly use products in our area of research and country. There is absolutely no conflict of interest between the authors and producers of the products because we do not intend to use these products as an avenue for any litigation but for the advancement of knowledge. Also, the research was not funded by the producing company rather it was funded by personal efforts of the authors.

COMPETING INTERESTS

Authors have declared that no competing interests exist.

REFERENCES

1. Naila A, Flint S, Fletcher G, Bremer P, Meerdink G. Control of biogenic amines in food - Existing and emerging approaches. J. Food Sci. 2010;75:139-150.
2. Lange J, Wittmann C. Enzyme sensor array for the determination of biogenic amines in food samples. Anal Bioanal Chem. 2002;372:276-283.
3. Stadnik J, Dolatowski ZJ. Biogenic amines in meat and fermented meat products. Acta Scientiarum Polonorum Technologia Alimentaria. 2010;9:251-263.
4. Kossel A. Üsber das agmatin. Von. 1910;257-261.
5. Regunathan S, Feinstein DL, Raasch W, Reis DJ. Agmatine (decarboxylated arginine) is synthesized and stored in astrocytes. Neuroreport. 1995;6:1897-1900.
6. Goracke-Postle CJ, Overland AC, Stone LS, Fairbanks CA. Agmatine transport into spinal nerve terminals is modulated by polyamine analogs. J. Neurochem. 2007;100:132-141.
7. Önal A, Tekkeli SEK, Önal C. A review of the liquid chromatographic methods for the determination of biogenic amines in foods. J. Food of Chem. 2013;138:509-515.
8. Sun X, Song W, Liu L. Enzymatic production of agmatine by recombinant arginine decarboxylase. J. Molecular Catalysis B: Enzymatic, 2015;121: 1-8.
9. Cabella C, Gardini G, Corpillo D. Transport and metabolism of agmatine in rat hepatocyte cultures. Eurpean J. of Biochem. 2001;268:940-947.
10. Alberto MR, Arena ME, De Nadra MCM. Putrescine production from agmatine by lactobacillus hilgardii: effet of phenolic compounds. Food Control. 2007;18:898-903.
11. Landette JM, Arena ME, Pardo I, De Nadra MCM, Ferrer S. Comparative survey of putrescine production from agmatine deamination in different bacteria. Food Microbiol. 2008;25:882-887.
12. Gilad GM, Gilad VH. Agmatine, and polyaminoguanidine-bound heterocyclic compounds for neurtrauma and neurodegenerative diseases. United States Patent 6114392. 2000;1-8.
13. Dreyfys JC. L'agmatine, un nouveau neurotransmetteur ? Medecine/sciences, 1994;10:589.
14. Li G, Regunathan S, Reis DJ. Agmatine is synthesized by a mitochondrial arginine decarboxylase in rat brain. Ann N Y Acad of Sci. 1995;763:325-329.
15. Reis DJ, Regunathan S. Is agmatine a novel neurotransmitter in Brain? Trends Pharmacol. Sci. 2000;21:187-93.
16. Halaris A, Plietz JJ. Agmatine Methabolic Pathwaye and spectrum of Activity in Brain. CNS Drugs, 2007; 21: 885-900.
17. Isome M, Lortie MJ, Murakami Y, Parisi E, Matsufuji S, Satriano J. The antiproliferative effects of agmatine correlate with the rate of cellular proliferation. J. Am. Physiol. Cell. Physiol. 2007;293:705-711.
18. Marx M, Trittenwein G, Aufrich C, Hoeger H, Lubec B. Agmatine and Spercmidine reduce collagen accumulation in kidneys of diabetic db/db mice. Nephron. 1995;65:155-158.
19. Mohseni G, Ostadhadi S, Imran-Khan M. Norouzi-Javidan A, Zolfaghari S, Haddadi N-S et al. Agmatine enhances the antidepressant-like effect of lithium in mouse forced swimming test through NMDA pathway. Biomed. and Pharmaco. 2017;88:931-938.
20. Kim JH, Kim JY, Mun CH, Suh M, Lee JE. Agmatine Modulates the Phenotype of Macrophage Acute Phase after Spinal Cord Injury in Rats. Experimental Neurobiol. 2017;26:278-286.
21. Gilad GM, Gilad VH. Long-term (5 years), high daily dosage of dietary agmatine-

evidence of safety: a case report. J Med. Food. 2014;17:1256-1259.

22. Eldeep GSS, Mokhtar SM, Mostafa GA, Taha RA, Gaballa AA. Relationship between Biogenic Amine Content and Hygienic Quality of Raw Meet in Fresh Fermented Sausage. J. Food Nutr. Disor. 2013;2:1-7.
23. Keynan O, Mirovsky Y, Dekel S, Gilad VH, Gilad GM. Safety and Efficacy of Dietary Agmatine Sulfate in Lumbar Disc-associated Radiculopathy. An Open-label, dose-escalating Study followed by a Randomized, Double-dlind, Placebo-controlled Trial. Pain Medicine. 2010;11:356-368.
24. Park JS, Lee CH, Kwon EY, Lee HJ, Kim JY, Kim SH. Monitoring the contents of biogenic amines in fish and fish products consumed in Korea. J. Food Control. 2010;21:1219-1226.
25. Shukla S, Park H-K, Kim J-K, Kim M. Determination of biogenic amines in Korean traditional fermented soybean paste (Doenjang). Food and Chem. Toxicol. 2010;48:1191-1195.
26. Redruello B, Ladero V, Del Rio B, Fernández M, Martin MC, Miguel A. A UHPLC method for the simultaneous analysis of biogenic amines, amino acids and ammonium ions in beer Alvarez. J. Food Chem. 2017;217:117-124.
27. Gardini F, Zaccarelli A, Belletti N, Faustini F, Cavazza A, Martuscelli M et al. Factors influencing biogenic amine production by a strain of Oenococcus oeni in a model system. Food Control. 2005;16:609-616.
28. Custódio FB, Tavares É, Glória MBA. Extraction of bioactive amines from grated Parmesan cheese using acid, alkaline and organic solvents. J. Food Composition and Analysis. 2007;20:280-288.
29. Novella-Rodríguez S, Veciana-Nogueés MT, Vidal-Carou MC. Biogenic Amines and Polyamines in Milks and Cheeses by Ion-Pair High Performance Liquid Chromatography. J. Agricultural Food Chem. 2000;48:5117-5123.
30. Kital K, Traoré M, Sarr D, Mbaye M, Mbaye O, Cisse L et al. Determination of Agmatine Rate by Spectrofluorimetric Method in Alkaline Medium: Optimization and Application on Shrimp. Journal of Chemistry and Biochemistry, 2019; 7: 15-26.
31. Nedeljko P, Turel M, Kosak A. Synthesis of hybrid thiol-functionalized SiO2 particles used for agmatine determination Aleksandra Lobnik1,2 J. Sol-Gel Sci. Technol. 2016;79:487-496.
32. Nedeljko P, Turel M, Lobnik A. Fluorescence-Based Determination of Agmatine in Dietary Supplements. Analytical Letters. 2015;48:1619-1628.
33. Özdestan Ö, Üren A. Biogenic amine content of kefir a fermented dairy product. European Food Research Technol. 2010;231:101-107.
34. Lapa-Guimarães J, Pickova J. New solvent systems for thin-layer chromatographic determination of nine biogenic amines in fish and squid. J. Chromatogr. A. 2004;1045:223-232.
35. Coly A, Aaron JJ. Simultaneous determination of sulfonylurea herbicide synthetic binary mixtures by a partial least square method combined with micellar-enhanced photochemically-induced fluorescence for application to tap water analysis. Maced. J. Chem. Chem. Eng. 2009;27:33-40.
36. Kital K, Traoré M, Sarr D, Mbaye M, Seye MDG, Coly A, et al. Thermodynamic and detailed kinetic study of the formation of orthophthalaldehyde-agmatine complex by fluorescence intensities. J. Analytical Sci. and Technol. 2020;11:1-13.
37. Simons SS. Jr., Johnson D. FReaction of o-Phthalaldeh yde and Thiols with Primary Amines: Formation of 1-Alkyl (and aryl) thio-2-alkylisoindoles. J. Org. Chem. 1978;43:2886-2891.
38. Aswad DW. Determination of D and L-Aspartate in amino acide mixtures by high-performance liquid chromatography after derivatization with a chiral adduct of o-phthaldialdehyde. Analytical Biochem. 1984;137:405-409.
39. Chen RF, Scott C, Trepman E. Fluorescence properties of O-phthaldialdehyde derivatives of amino acids. Biochimica et biophysica acta, 1979;576:440-455.
40. Alvarez-Coque MCG, Hernhdez MJM, Camaiias RMV. Formation and Instability o-Phthalaldehyde Derivatives of Amino Acids. Analytical Biochemistry, 1989; 178:1-7.

41. Imai K, Toyo'oka T, Miyano H. Fluorigenic reagents for primary and secondary amines and thiols in high-performance liquid chromatography. Analyst. 1984; 109:1365-1373.

42. Albarrcin W, Sanchez IC, Gau R, Barat JM. Salt in food processing; usage and reduction: a review. Intern. J. Food Sci. and Technol. 2011;46:1329-1336.

Peer-review history:
The peer review history for this paper can be accessed here:
http://www.sdiarticle4.com/review-history/75576